

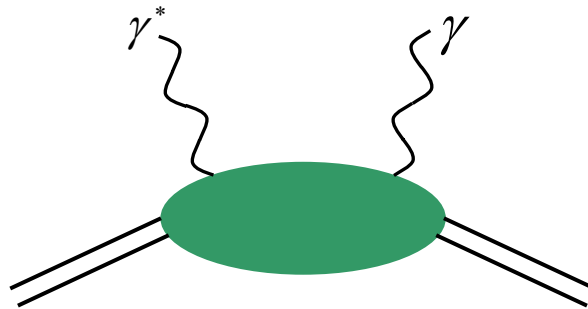
Deeply Virtual Compton Scattering

(e,e'N γ) Experiments @ JLab - Hall A

Eric Voutier

for the Jefferson Lab Hall A and DVCS Collaborations

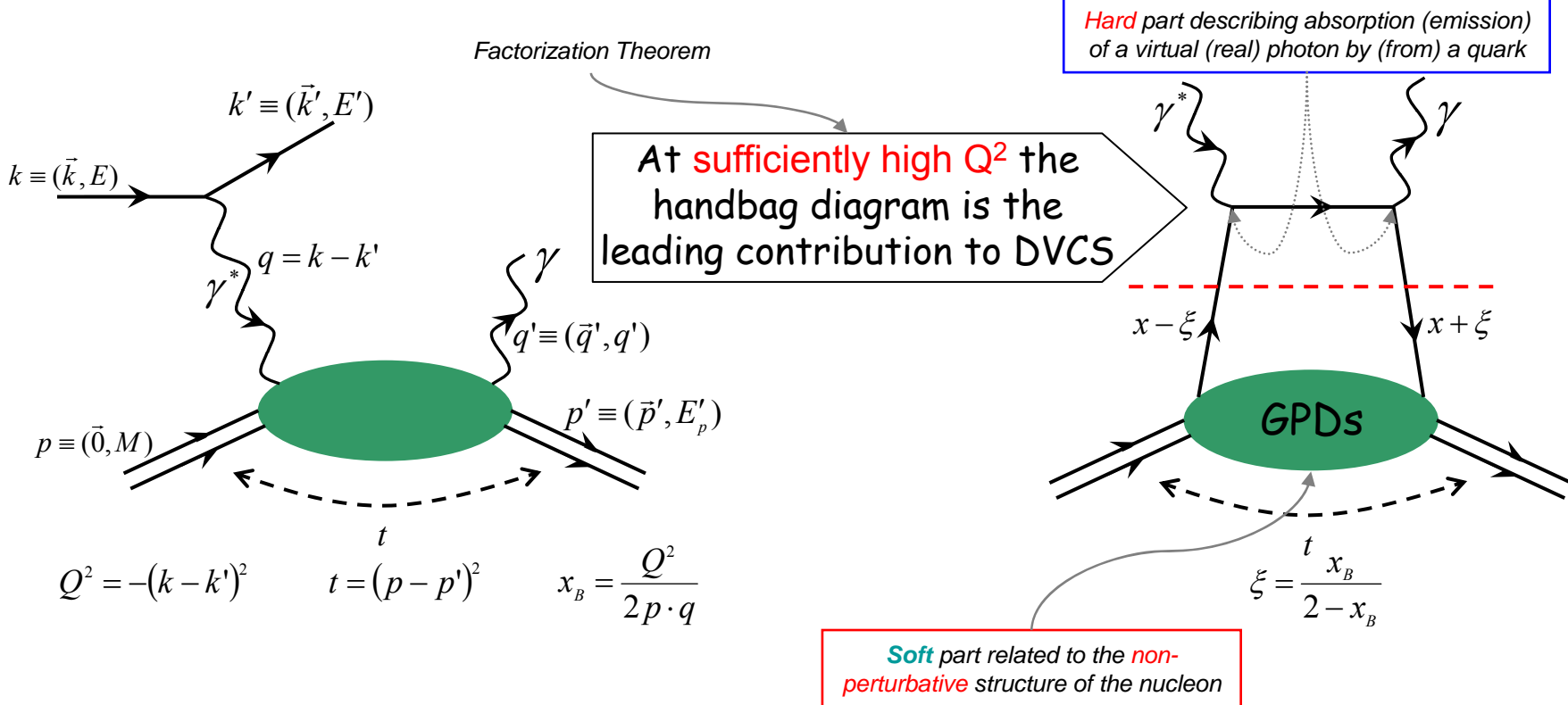
*Laboratoire de Physique Subatomique et de Cosmologie
Grenoble, France*



- (i) DVCS & GPDs
- (ii) Experimental features
- (iii) p-DVCS @ JLab.Hall_A
- (iv) n-DVCS @ JLab.Hall_A
- (v) Future Prospects
- (vi) Conclusions

The DVCS Process

DVCS is the simplest process to access Generalized Parton Distributions



X. Ji, J. Osborne, PRD 58 (1998) 094018

J.C. Collins, A. Freund, PRD 59 (1999) 074009

DVCS & GPDs (I)

The GPDs Framework

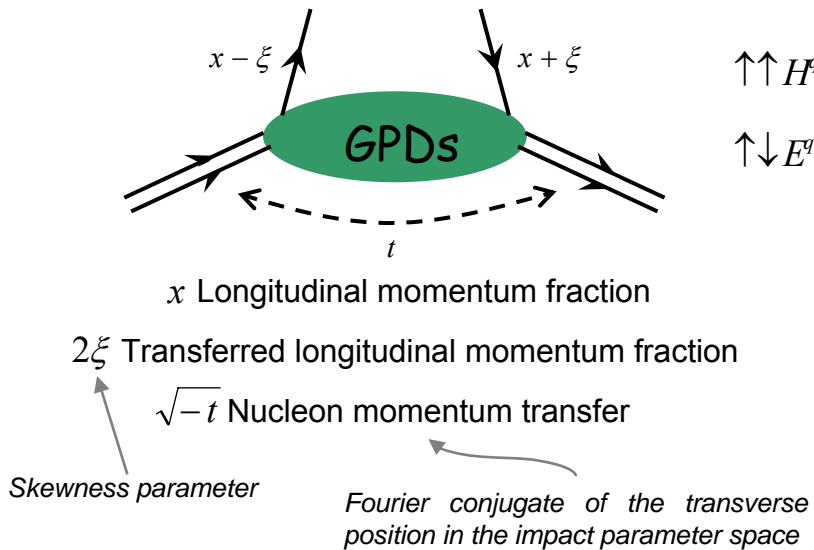
D. Müller et al., FP 42 (1994) 101

A.V. Radyushkin, PRD 56 (1997) 5524

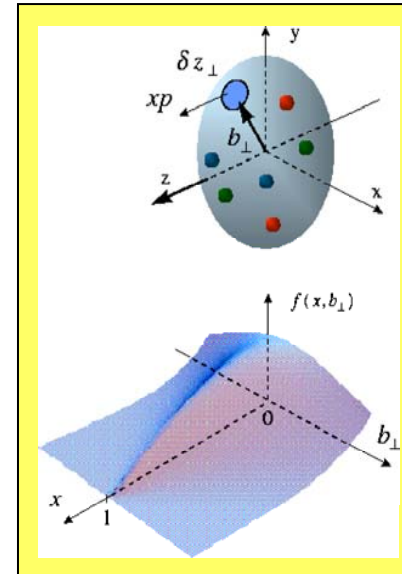
X. Ji, PRL 78 (1997) 610

At leading order, **GPDs** are 4 universal parton distributions (+4 gluon GPDs) describing the nucleon structure

Coherence between quantum states of different **helicity**, **longitudinal momentum** and **transverse position**



$$\begin{array}{ll} \uparrow\uparrow H^q(x, \xi, t) & \downarrow\downarrow \tilde{H}^q(x, \xi, t) \\ \uparrow\downarrow E^q(x, \xi, t) & \downarrow\uparrow \tilde{E}^q(x, \xi, t) \end{array}$$



M. Burkardt, PRD 62 (2000) 071503 M.Diehl, EPJC 25 (2002) 223

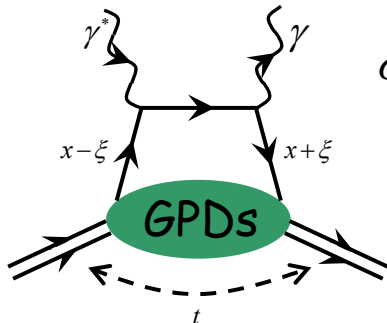
1/Q resolution distribution in the transverse plane of partons with longitudinal momentum x

$$J^q = \frac{1}{2} \Delta \Sigma + L^q = \frac{1}{2} \int_{-1}^{+1} dx \ x \ [H^q(x, \xi, t=0) + E^q(x, \xi, t=0)]$$

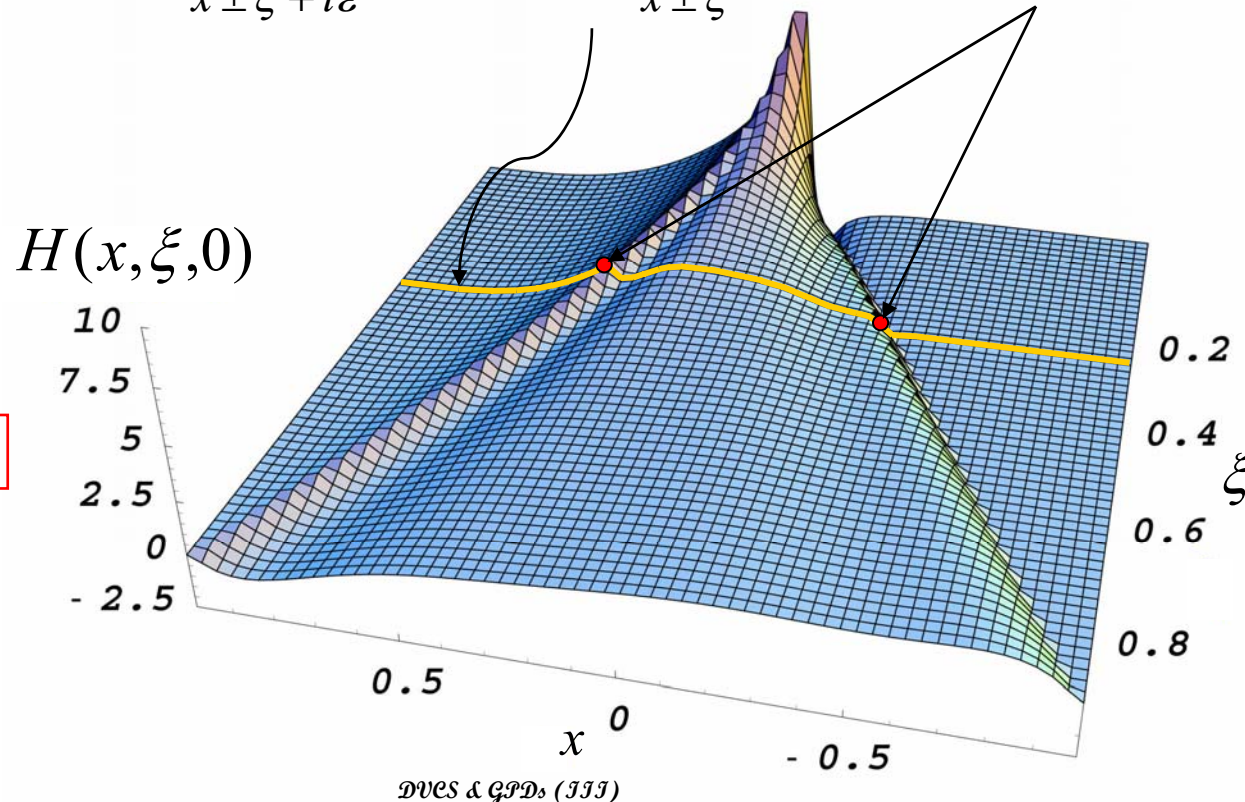
Deep Exclusive Scattering

GPDs can be accessed via **exclusive reactions** in the **Bjorken kinematic regime**

GPDs enter the **cross section** of hard scattering processes via an **integral** over the intermediate quarks longitudinal momenta

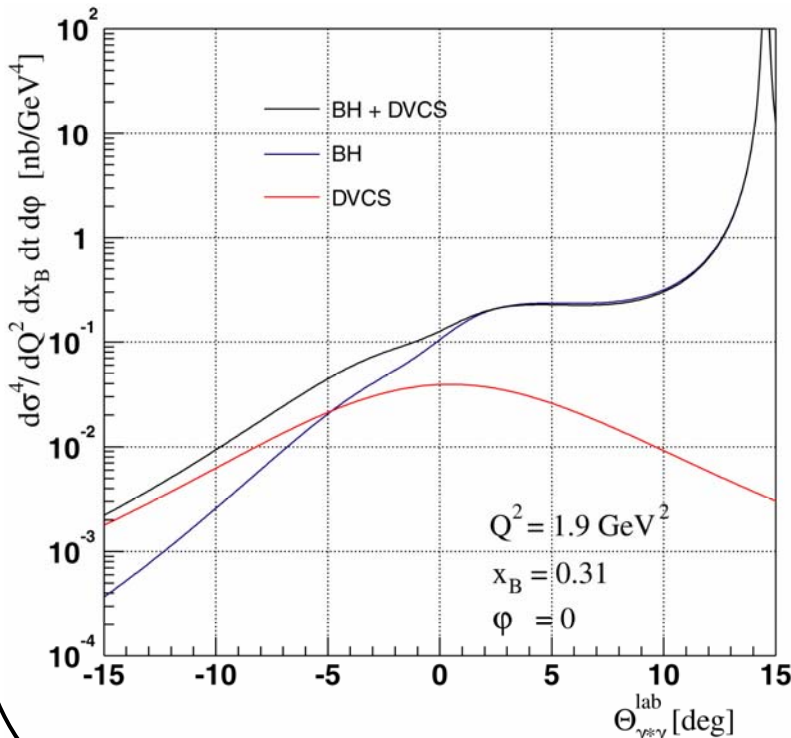
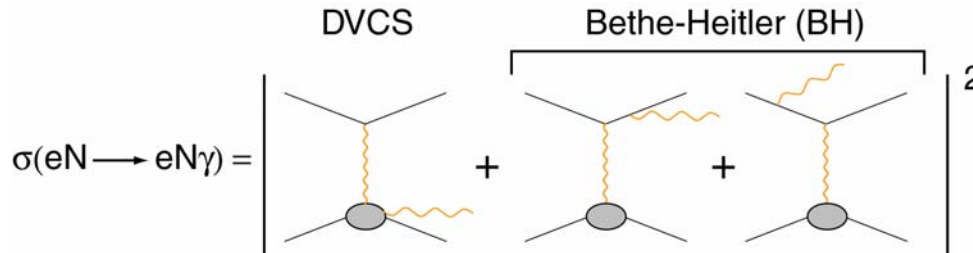


$$\sigma \propto \int_{-1}^{+1} dx \frac{GPD(x, \xi, t)}{x \pm \xi \mp i\epsilon} = \mathcal{P} \int_{-1}^{+1} dx \frac{GPD(x, \xi, t)}{x \pm \xi} \pm i\pi GPD(x = \pm \xi, \xi, t)$$



$Q^2 \gg M^2$ - $t \ll Q^2$

Photon Electroproduction



P. Kroll, P.A.M. Guichon, M. Diehl, B. Pire, M. Vanderhaeghen...

DVCS & GPDs (IV)

DVCS & Bethe-Heitler processes are undistinguishable
BUT the Bethe-Heitler amplitude is calculable and known at low t

Unpolarized Cross Section

$$\frac{d^5\sigma}{dQ^2 dx_B dt d\phi_e d\varphi} = \mathcal{T}_{BH}^2 + |\mathcal{T}_{DVCS}|^2 - 2 \frac{e}{|e|} \cdot \mathcal{T}_{BH} \cdot \Re \{ \mathcal{T}_{DVCS} \}$$

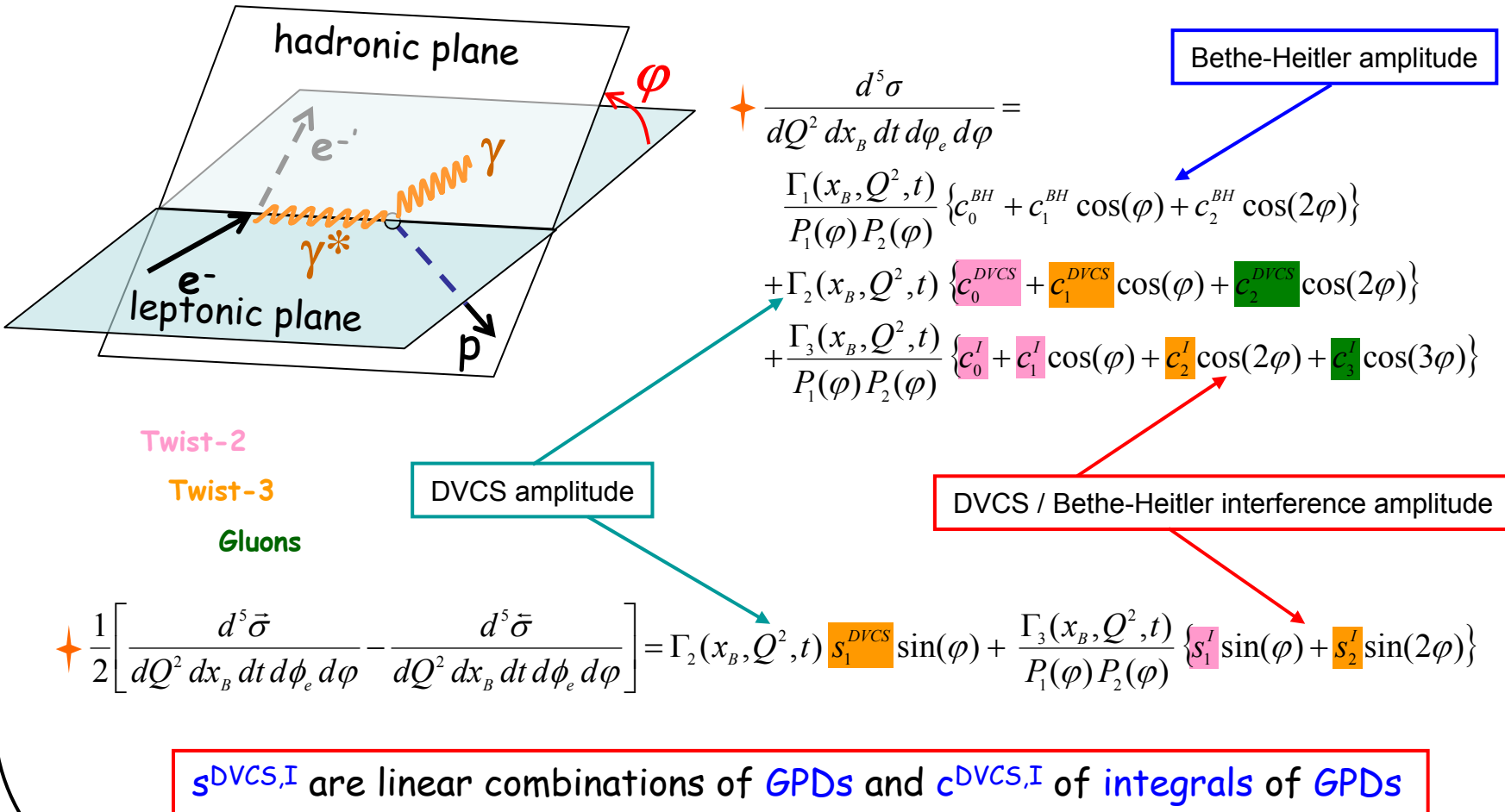
Lepton beam charge

Polarized Cross Section Difference

$$\begin{aligned} & \frac{1}{2} \left[\frac{d^5\bar{\sigma}}{dQ^2 dx_B dt d\phi_e d\varphi} - \frac{d^5\bar{\sigma}}{dQ^2 dx_B dt d\phi_e d\varphi} \right] \\ &= \mathcal{T}_{BH} \cdot \Im \{ \mathcal{T}_{DVCS} \} + \Re \{ \mathcal{T}_{DVCS} \} \cdot \Im \{ \mathcal{T}_{DVCS} \} \end{aligned}$$

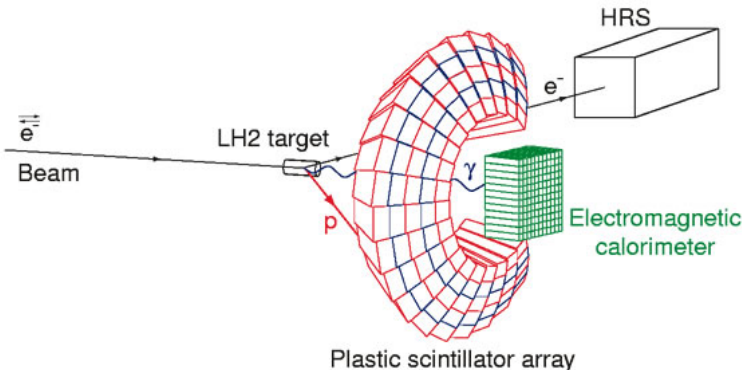
DVCS Harmonic Structure

A.V. Belitsky, D. Müller, A. Kirchner, NPB 629 (2002) 323



DVCS @ JLab.Hall_A

Dedicated High Precision Experiment



p-DVCS

Test of handbag dominance between 1.5 and 2.3 GeV^2 in the valence region
Mostly sensitive to \mathcal{H}

n-DVCS

Exploratory measurement of the polarized cross section difference at 1.9 GeV^2 in the valence region
Mostly sensitive to \mathcal{E}

An experimental challenge

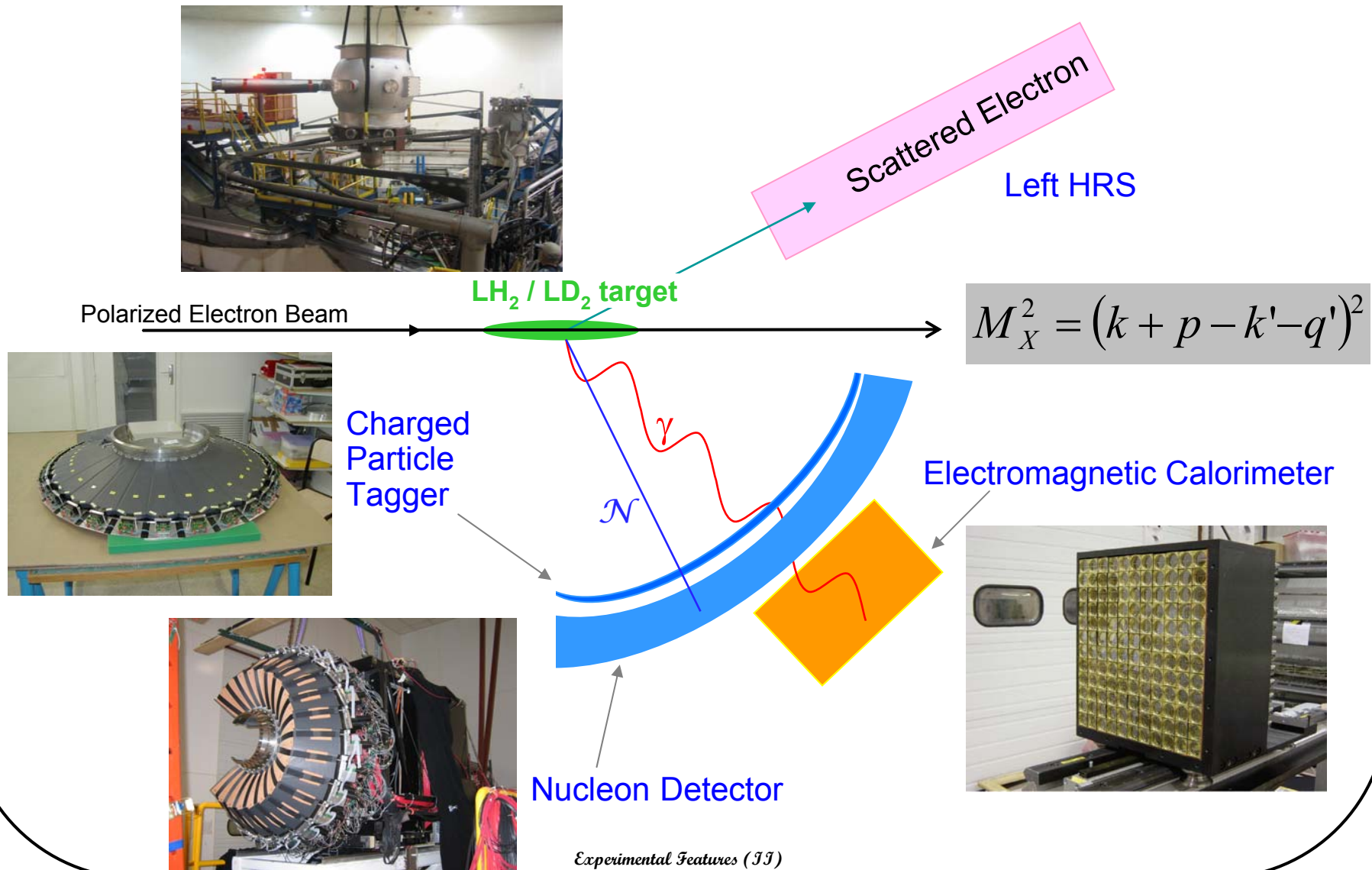
- ❖ Large luminosity
 $4 \mu\text{A}$ onto 15 cm LD₂ **$4 \cdot 10^{37} \text{ cm}^{-2} \cdot \text{s}^{-1}$ /nucleon**
- ❖ Direct view & vicinity of the target
within **60 cm** to **1 m** from the interaction vertex
at **forward angles**
- ❖ Hostile electromagnetic ambiance
large background from Møller electrons



Specific Scattering Chamber
Čerenkov based Electromagnetic Calorimeter
Customized Electronics & Data Acquisition

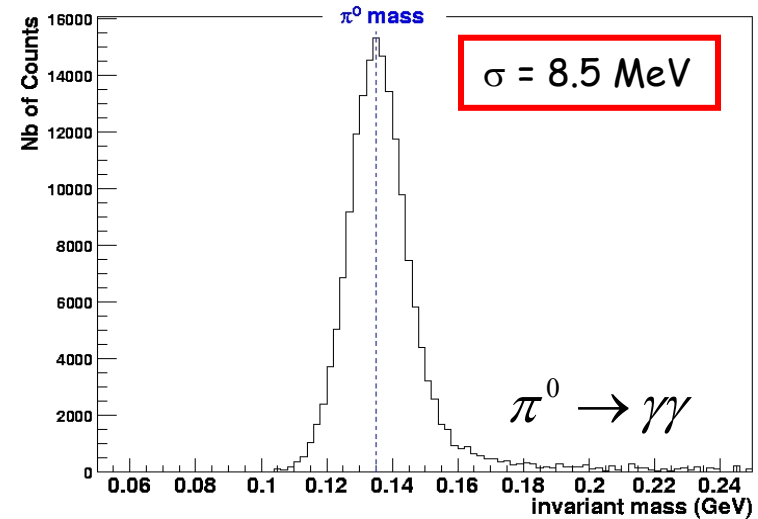
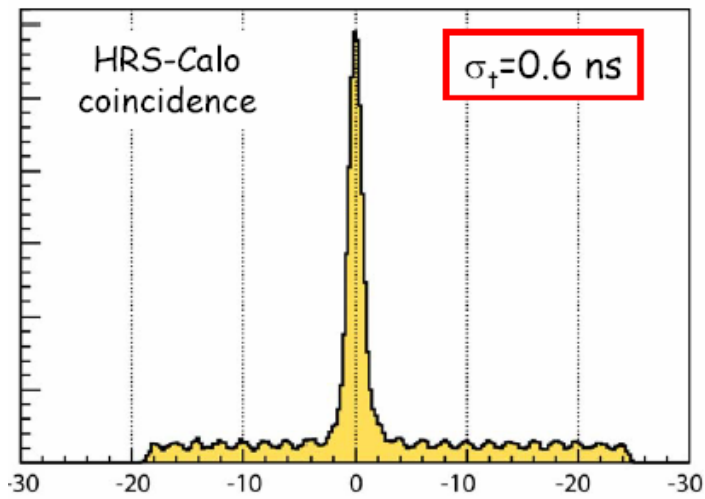
Experimental Features (I)

Experimental Apparatus



DVCS Setup Performances

Electromagnetic Calorimeter



The electromagnetic calorimeter is calibrated with $H(e, e_{\text{Calo}}, p_{\text{HRS}})$ elastic scattering

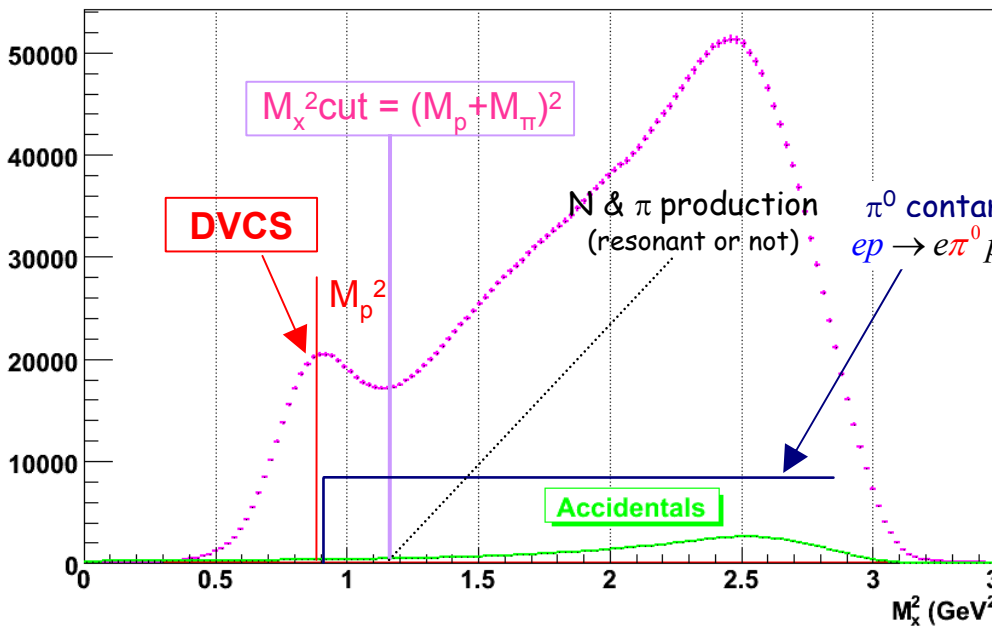
The monitoring of the calibration coefficient is insured via π^0_{Calo} , π^-_{HRS} detection and a relative procedure based on aging from radiation exposure

$$\delta t < 1 \text{ ns}$$

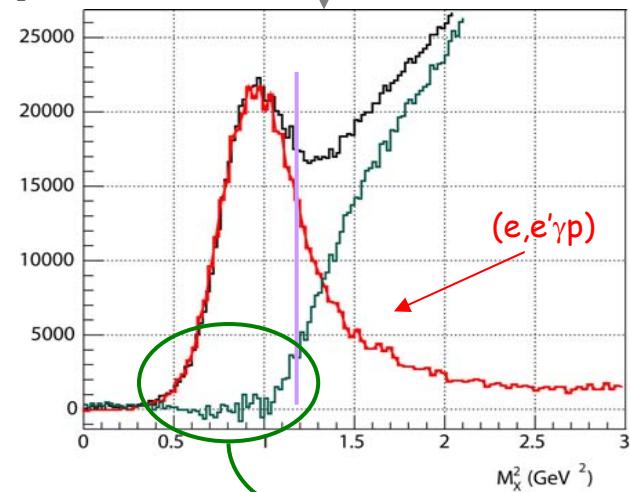
$$\delta E/E = 2.5 \% \text{ at } 4.2 \text{ GeV}$$

$$\delta x = \delta y = 2 \text{ mm}$$

Experimental Exclusivity



Subtraction of π^0 contamination (1 γ in the calorimeter) is obtained from a phase space simulation which weight is adjusted to the experimental π^0 cross section (2 γ in the calorimeter).

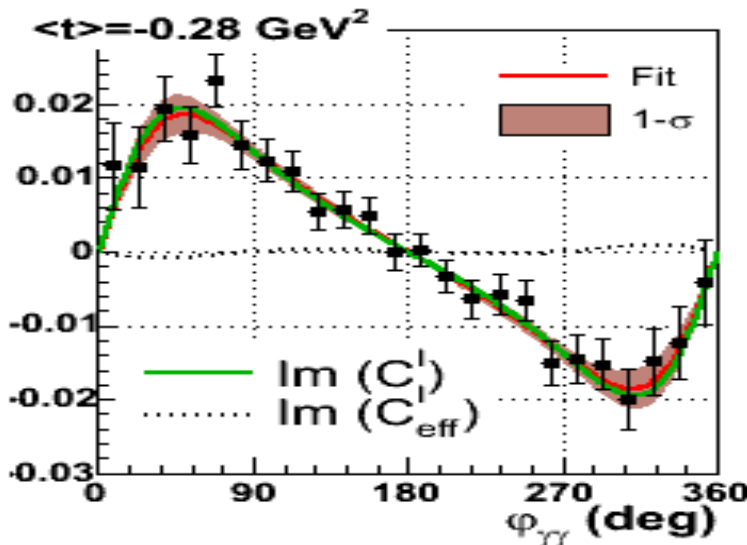


Remaining contribution < 3 %
(all non- π^0 electroproduction)

E00-110 → p -DVCs

P.Y. Bertin, C.E. Hyde-Wright, R. Ransome, F. Sabatié *et al.*

Beam Polarized Cross Section Difference



Harmonic coefficients are obtained via a minimization procedure between experimental and Monte Carlo simulated yields taking into account real external and internal radiative corrections, resolution and acceptance effects

$$\chi^2 = \sum_{i_e} \frac{[\Delta N^{\text{Exp}}(i_e) - \Delta N^{\text{MC}}(i_e)]^2}{[\delta N^{\text{Exp}}(i_e)]^2}$$

$\star \frac{1}{2} \left[\frac{d^5 \bar{\sigma}}{dQ^2 dx_B dt d\phi_e d\varphi} - \frac{d^5 \bar{\sigma}}{dQ^2 dx_B dt d\phi_e d\varphi} \right] =$
 $\Gamma_2(x_B, Q^2, t) s_1^{DVCS} \sin(\varphi) + \frac{\Gamma_3(x_B, Q^2, t)}{P_1(\varphi) P_2(\varphi)} \left(s_1^I \sin(\varphi) + s_2^I \sin(2\varphi) \right)$

 $s_1^I = 8Ky(2-y) \operatorname{Im}\{C^I(\mathcal{F})\}$

 $C^I(\mathcal{F}) = F_1(t) \mathcal{H} + \xi(F_1(t) + F_2(t)) \tilde{\mathcal{H}} - \frac{t}{4M^2} F_2(t) \mathcal{E}$

 $\operatorname{Im}\{\mathcal{H}\} = \pi \sum_q e_q^2 \left\{ H^q(\xi, \xi, t) - H^q(-\xi, \xi, t) \right\}$

 GPD

s_1^I Twist-2 (BH.DVCS interference)
 s_2^I Twist-3 (BH.DVCS interference)
 ~~s_1^{DVCS}~~ Twist-3 (DVCS,DVCS)

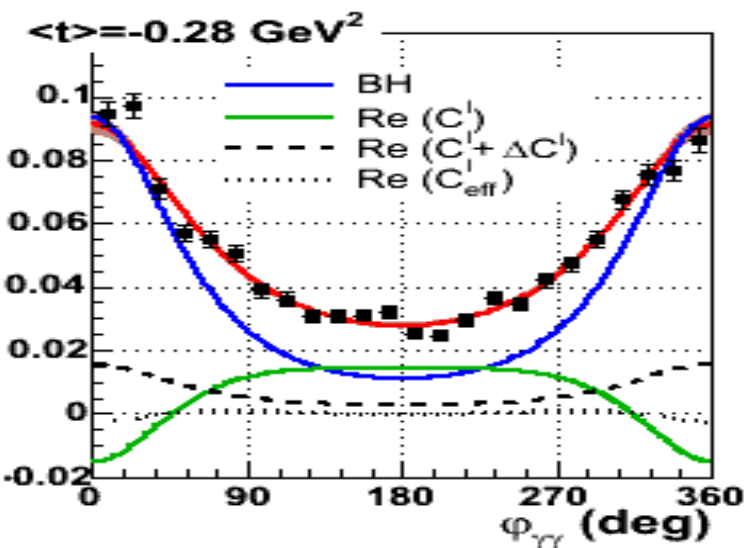
Unpolarized Cross Section

$$\begin{aligned}
 \frac{d^5\sigma}{dQ^2 dx_B dt d\varphi_e d\varphi} = & \frac{\Gamma_1(x_B, Q^2, t)}{P_1(\varphi) P_2(\varphi)} \left\{ c_0^{BH} + c_1^{BH} \cos(\varphi) + c_2^{BH} \cos(2\varphi) \right\} + \Gamma_2(x_B, Q^2, t) \left\{ c_0^{DVCS} + c_1^{DVCS} \cos(\varphi) + c_2^{DVCS} \cos(2\varphi) \right\} \\
 & + \frac{\Gamma_3(x_B, Q^2, t)}{P_1(\varphi) P_2(\varphi)} \left\{ c_0^I + c_1^I \cos(\varphi) + c_2^I \cos(2\varphi) + c_3^I \cos(3\varphi) \right\}
 \end{aligned}$$

BH.BH amplitude BH.DVCS interference DVCS.DVCS amplitude

c_0^I Twist-2 (BH.DVCS interference)
 c_1^I Twist-2 (BH.DVCS interference)
 c_2^I Twist-3 (BH.DVCS interference)
 ~~c_3^I Gluon Contribution (BH.DVCS interference)~~

c_0^{DVCS} Twist-2 (DVCS.DVCS)
 c_1^{DVCS} Twist-3 (DVCS.DVCS)
 ~~c_2^{DVCS} Gluon Contribution (DVCS.DVCS)~~



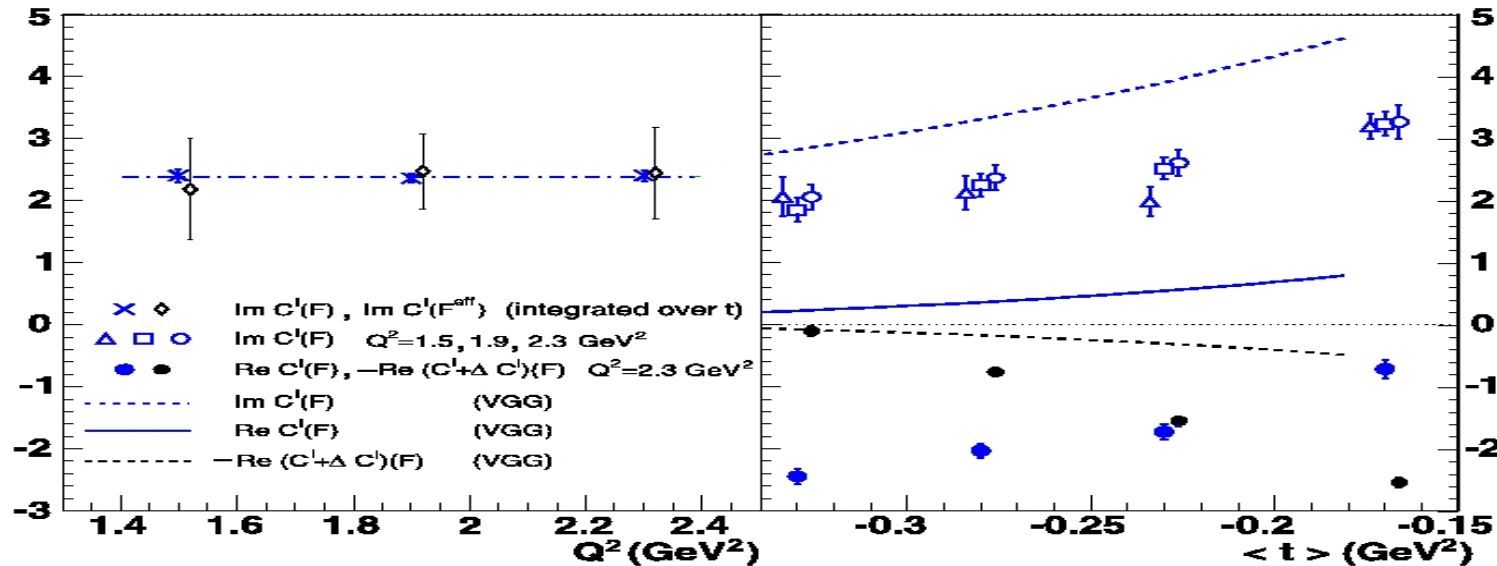
C. Muñoz-Camacho, Doctorat Thesis, Saclay, 2005

 p -DVCS @ JLab.Hall-A (JII)

$$\begin{aligned}
 \Rightarrow C^I(\mathcal{F}) &= F_1(t) \mathcal{H} + \xi(F_1(t) + F_2(t)) \tilde{\mathcal{H}} - \frac{t}{4M^2} F_2(t) \mathcal{E} \\
 \Rightarrow C^I(\mathcal{F}) + \Delta C^I(\mathcal{F}) &= \\
 F_1(t) \mathcal{H} - \frac{t}{4M^2} F_2(t) \mathcal{E} - \xi^2(F_1(t) + F_2(t)) (\mathcal{H} + \mathcal{E}) &
 \end{aligned}$$

$\tilde{\mathcal{H}}$ Independent linear combination

Experimental Results



- ❖ Twist-two contributions **dominate** the DVCS cross section and are **Q^2 independent** in the measured kinematics range
- ❖ Twist-three contributions to cross section are **small** and are **Q^2 independent** within error bars
- ❖ The t dependence of each harmonic coefficient is **consistent with expectations** while their values are not reproduced by models

↓

Strong indication for handbag dominance at Q^2 about 2 GeV^2 in the valence region

E03-106 → $n\text{-DVCS}$

P.Y. Bertin, C.E. Hyde-Wright, F. Sabatié, E. Voutier *et al.*

Neutron targets allow to access the least known and constrained GPD

$$C_n(\mathcal{F}) = F_1(t) \mathcal{H} + \xi(F_1(t) + F_2(t)) \tilde{\mathcal{H}} - \frac{t}{4M^2} F_2(t) \mathcal{E}$$

Suppressed because $F_1(t)$ is small

Suppressed because of cancellation between u and d quarks

	s (GeV ²)	Q ² (GeV ²)	P _e (Gev/c)	Θ _e (deg)	-Θ _{γ*} (deg)	∫ Ldt (fb ⁻¹)
Hydrogen	4.22	1.91	2.95	19.32	18.25	4365
Deuterium	4.22	1.91	2.95	19.32	18.25	24000

Neutron data $n(e, e'\gamma)$ are obtained from the comparison between deuterium $D(e, e'\gamma)$ and hydrogen data $H(e, e'\gamma)$

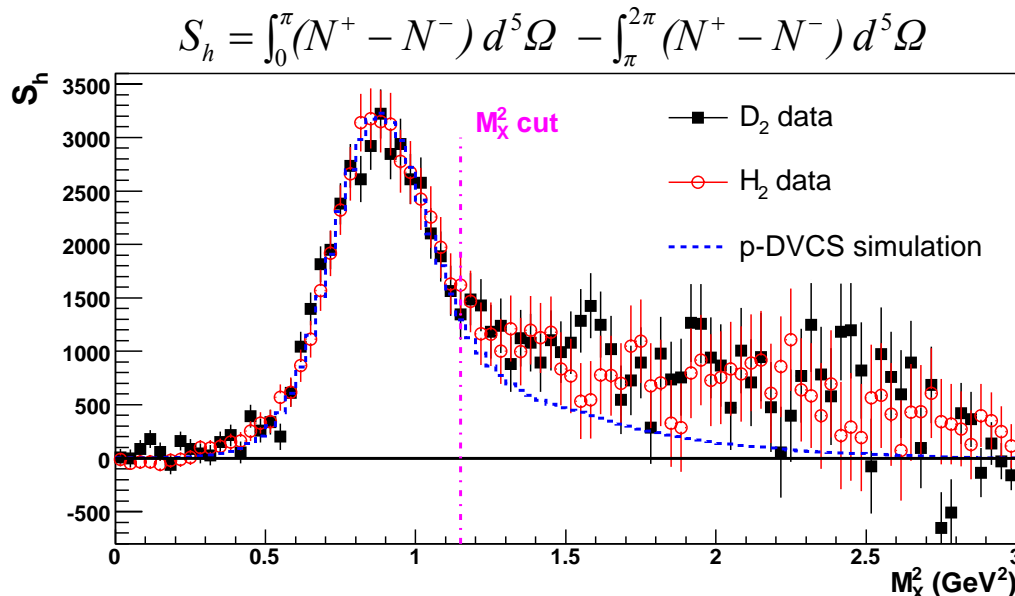
$$D(e, e'\gamma)X = p(e, e'\gamma)p + n(e, e'\gamma)n + d(e, e'\gamma)d + \dots$$

Subtraction of quasi-elastic proton contribution deduced from H^2 data convoluted with the initial motion of the nucleon

$$M_X^2 = (q + p - q')^2 - 2\vec{p}_i \cdot (\vec{q} - \vec{q}')$$

Dynamical separation of quasi-elastic neutron and elastic deuteron contributions

$$M_X^2(H_2) - M_X^2(D_2) = t/2$$



From a sample of high energy π^0

$$\frac{N_{\pi^0}(D_2)}{N_{\pi^0}(H_2)} = 0.95 \pm 0.06$$

π^0 contamination **cancels** in the subtraction method

Beam Polarized Cross Section Difference

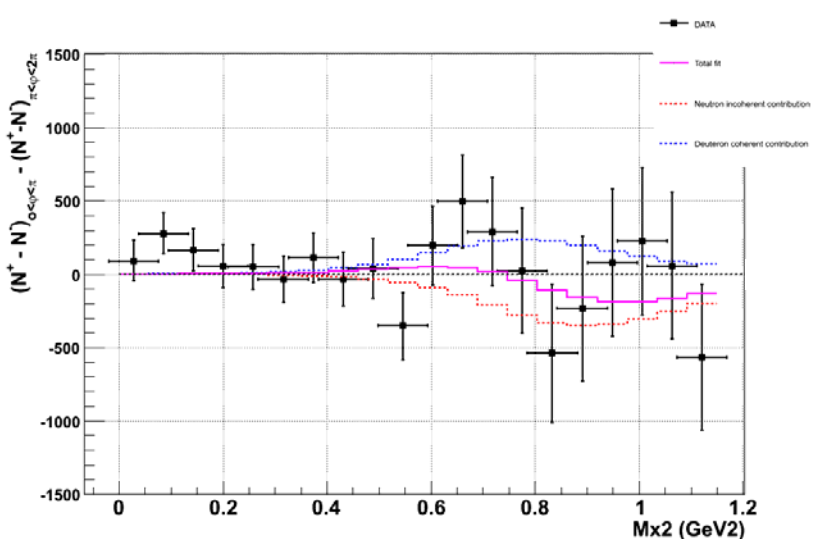
$$\frac{1}{2} \left[\frac{d^5 \vec{\sigma}}{dQ^2 dx_B dt d\phi_e d\varphi} - \frac{d^5 \bar{\sigma}}{dQ^2 dx_B dt d\phi_e d\varphi} \right] = \Gamma_{2n}(x_B, Q^2, t) s_{1n}^{DVCS} \sin(\varphi) + \frac{\Gamma_{3n}(x_B, Q^2, t)}{P_{1n}(\varphi) P_{2n}(\varphi)} \{s_{1n}^I \sin(\varphi) + s_{2n}^I \sin(2\varphi)\}$$

$$+ \Gamma_{2d}(x_B, Q^2, t) s_{1d}^{DVCS} \sin(\varphi) + \frac{\Gamma_{3d}(x_B, Q^2, t)}{P_{1d}(\varphi) P_{2d}(\varphi)} \{s_{1d}^I \sin(\varphi) + s_{2d}^I \sin(2\varphi)\}$$

Neutron contribution Deuton contribution

~~s_{1n}^I Twist-2 (BH.DVCS interference)~~
 ~~s_{2n}^I Twist-3 (BH.DVCS interference)~~
 ~~s_{1n}^{DVCS} Twist-3 (DVCS.DVCS)~~

~~s_{1d}^I Twist-2 (BH.DVCS interference)~~
 ~~s_{2d}^I Twist-3 (BH.DVCS interference)~~
 ~~s_{1d}^{DVCS} Twist-3 (DVCS.DVCS)~~

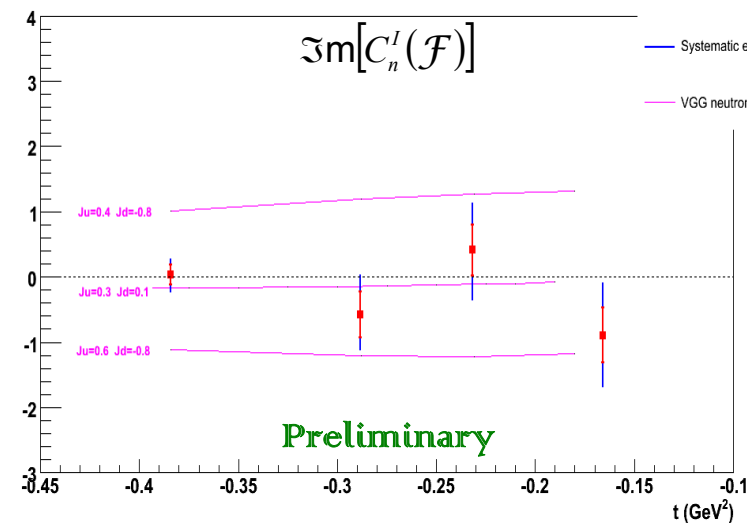
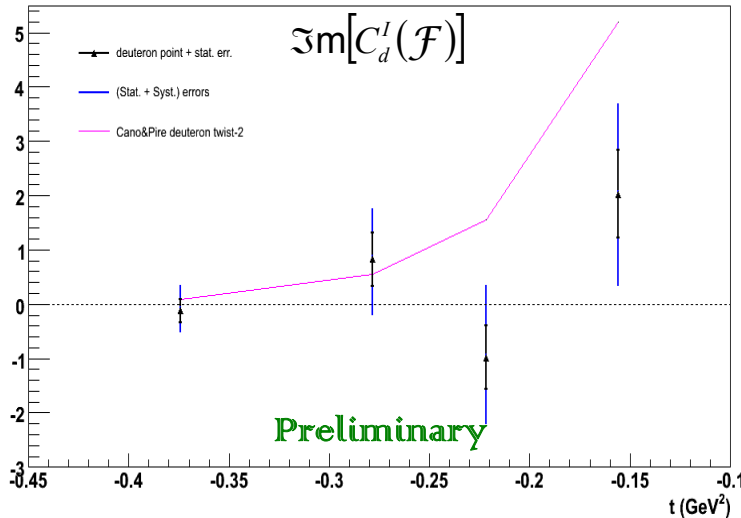


$$\Rightarrow C_n^l(\mathcal{F}) = F_1(t) \mathcal{H} + \xi(F_1(t) + F_2(t)) \tilde{\mathcal{H}} - \frac{t}{4M^2} F_2(t) \mathcal{E}$$

$$\Rightarrow C_d^l(\mathcal{F}) = (\mathcal{H}_1 \cdots \mathcal{H}_5 \tilde{\mathcal{H}}_1 \cdots \tilde{\mathcal{H}}_4) \mathcal{M} \begin{pmatrix} G_1 \\ G_2 \\ G_3 \end{pmatrix}$$

Experimental Results

$x_B = 0.36 \quad Q^2 = 1.91 \text{ GeV}^2$

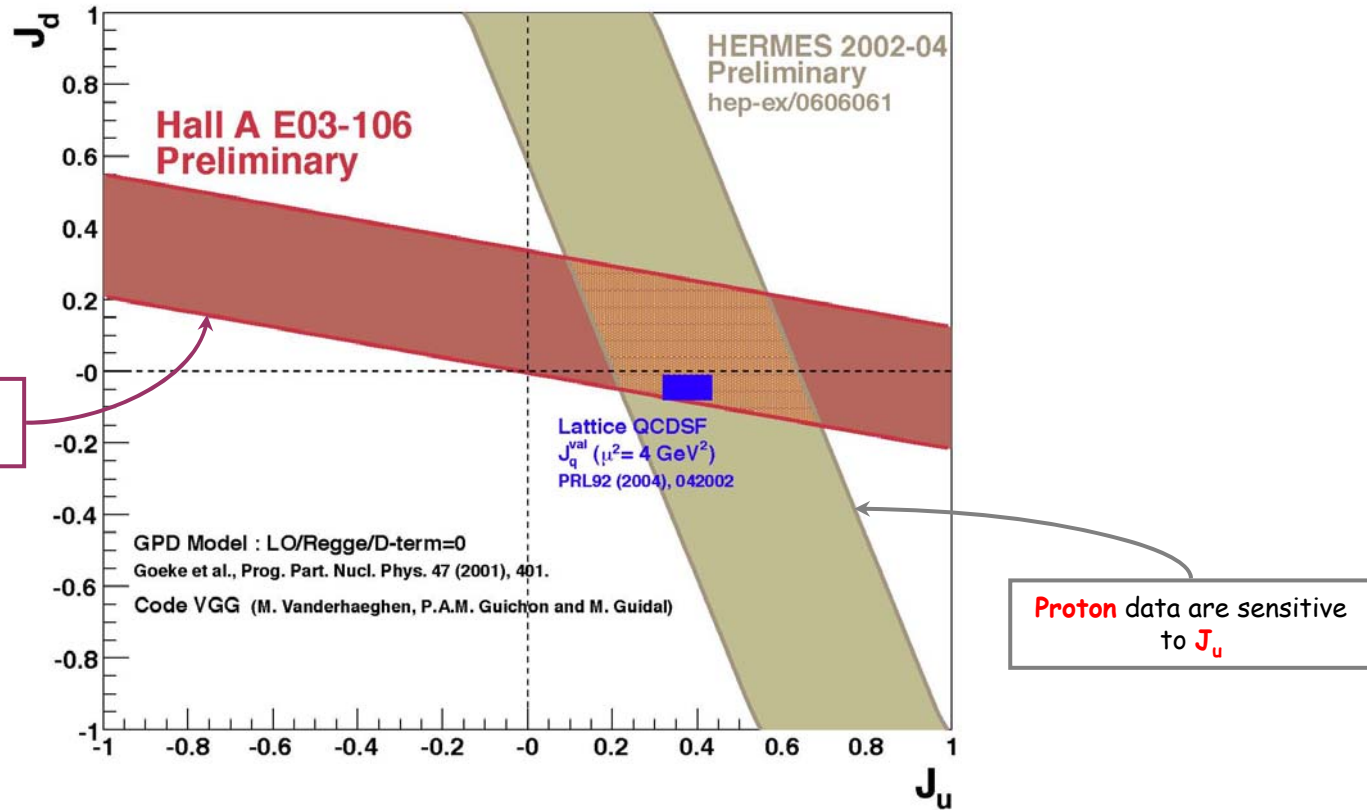


- ❖ Indication for two contributions of opposite signs
- ❖ Deuteron moments are **poorly defined** by these data; exploration of small $|t|$ region might be an **opportunity** for future experiments
- ❖ Neutron moments are **small** and compatible with zero; the measured t evolution provides **constraints** on GPD models

Model Dependent Quark Angular Momenta

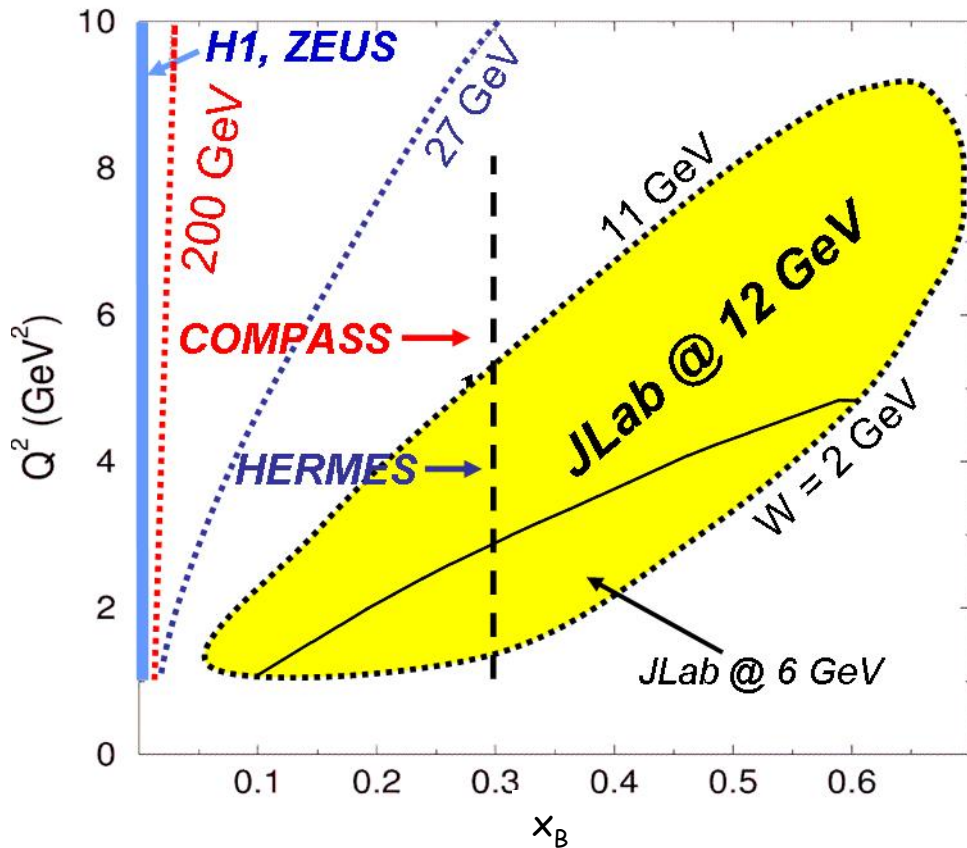
F. Ellinghaus et al., EPJ C46 (2006) 729

$$\chi^2_{\min} \leq \chi^2(J_u, J_d) = \sum_i \frac{\left(\Im m[C_n^I(\mathcal{F})]_{VGG}^{\exp}(t_i) - \Im m[C_n^I(\mathcal{F})]_{VGG}^{J_u, J_d}(t_i) \right)^2}{[\delta_{\text{stat}}^{\exp}(t_i)]^2 + [\delta_{\text{syst}}^{\exp}(t_i)]^2} \leq \chi^2_{\min} + 1$$



Complementarity between neutron and transversally polarized proton measurements

GPDs @ JLab 12 GeV



The **energy upgrade** of the CEBAF accelerator allows access to the **high x_B** region which requires **large luminosity**

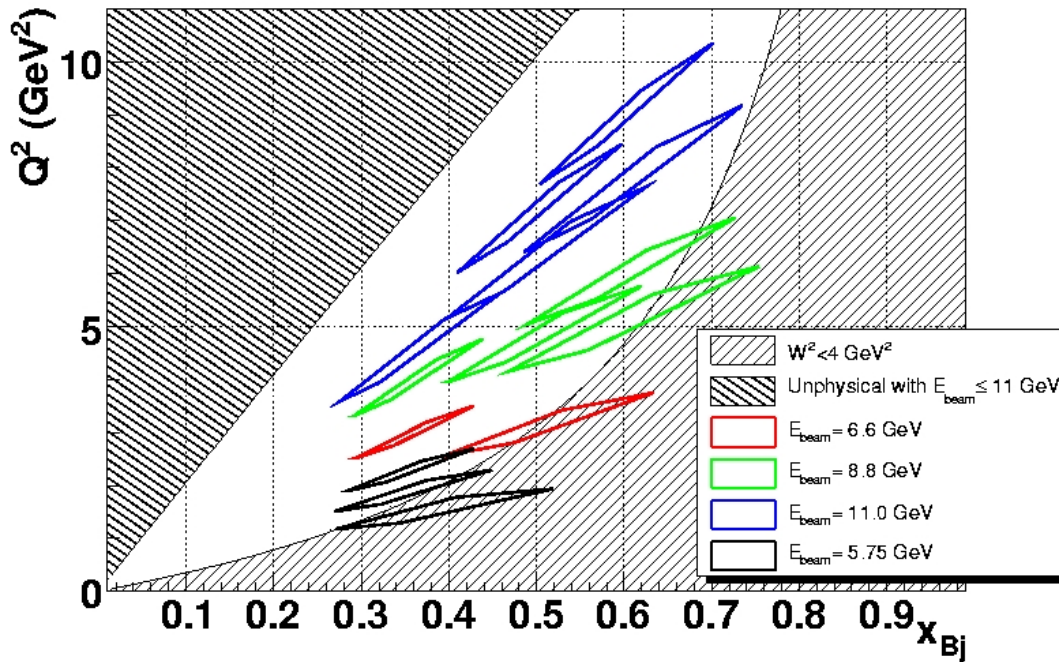
Specific DVCS cross section studies in Hall A

DVCS, DDVCS & DVMP measurements over a large kinematic domain in Hall B with CLAS12

$E12-06-114 \rightarrow p\text{-DVCS}$

C. Hyde-Wright, B. Michel, C. Muñoz Camacho, J. Roche *et al.*

DVCS measurements in Hall A/JLab



High precision cross section data in selected regions of the phase space

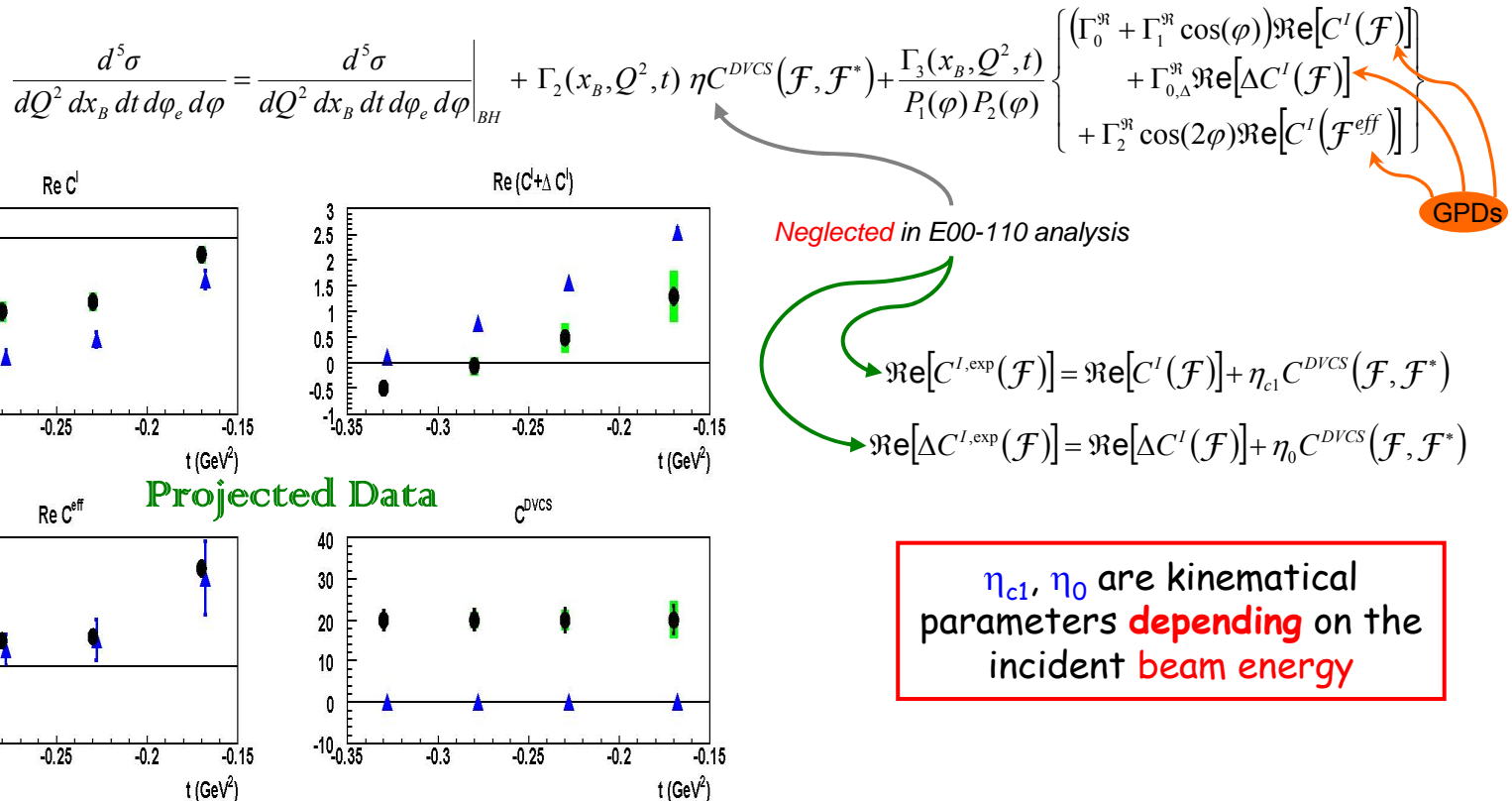
High Resolution Spectrometers
Upgraded DVCS calorimeter

Measurement of polarized & unpolarized p-DVCS cross sections
Extension to the neutron cross sections & recoil nucleon polarization observables
Possible extensions with polarized targets (?) & positron beam (?)

E07-007 → p-DVCS²

P.Y. Bertin, C. Hyde-Wright, C. Muñoz Camacho, J. Roche *et al.*

Rosenbluth like investigation of the DVCS cross section off the proton



Study of the importance of DVCS bilinear contribution to the cross section

Summary

... Too Early to Conclude ...

The dominance of the handbag mechanism in DVCS was observed at Q^2 as low as 2 GeV 2 , validating GPD like analysis at JLab energies

First measurements of DVCS off the neutron confirm the expected sensitivity to E

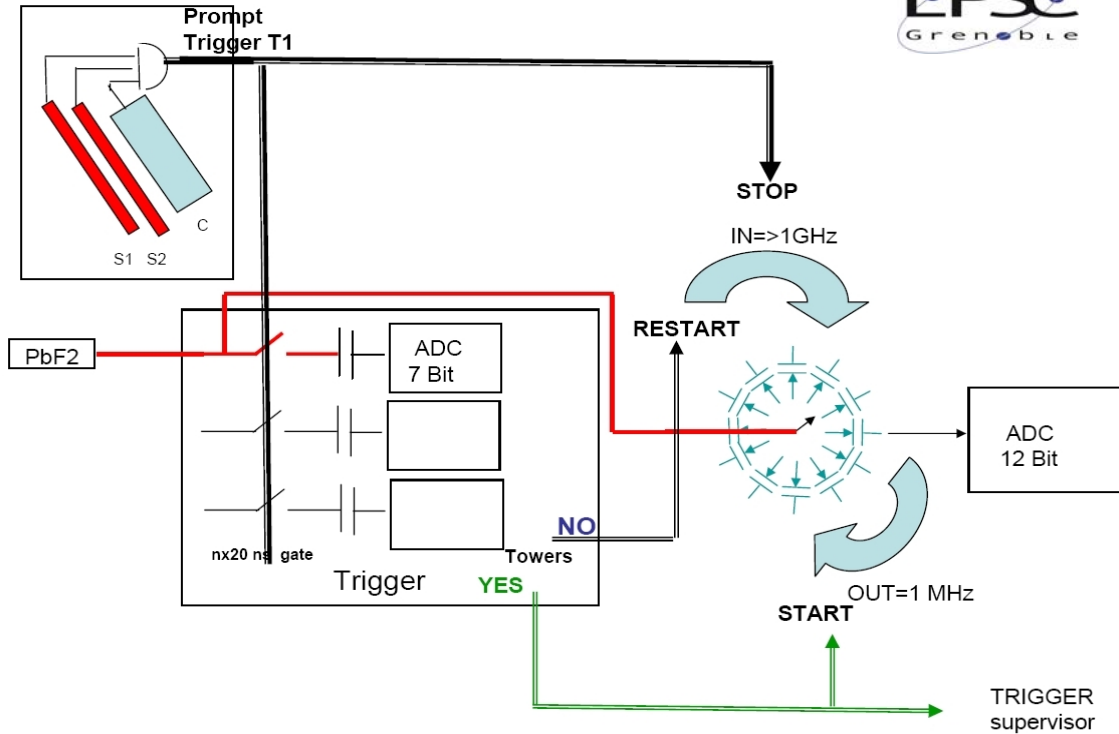
Neutron experiments are mandatory complements to proton ones

DVCS @ JLab.Hall_A continues at 6 and 12 GeV with an upgraded calorimeter (acceptance, trigger...) towards detailed investigations and exhaustive mapping of GPDs

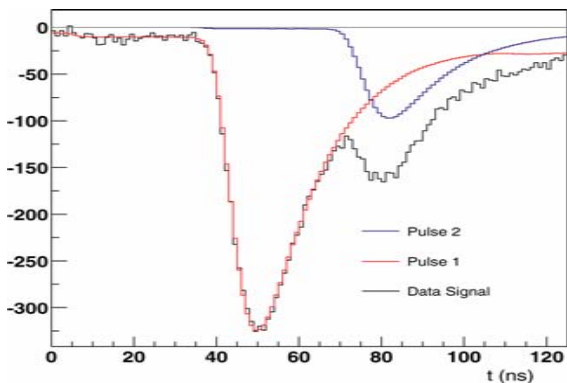
DVCS DVMP

Conclusions (I)

Fast Trigger



Signal Sampling



Registering of any group of **4 neighbouring blocks** is enabled when the energy deposit in this group exceeds a fixed **threshold**

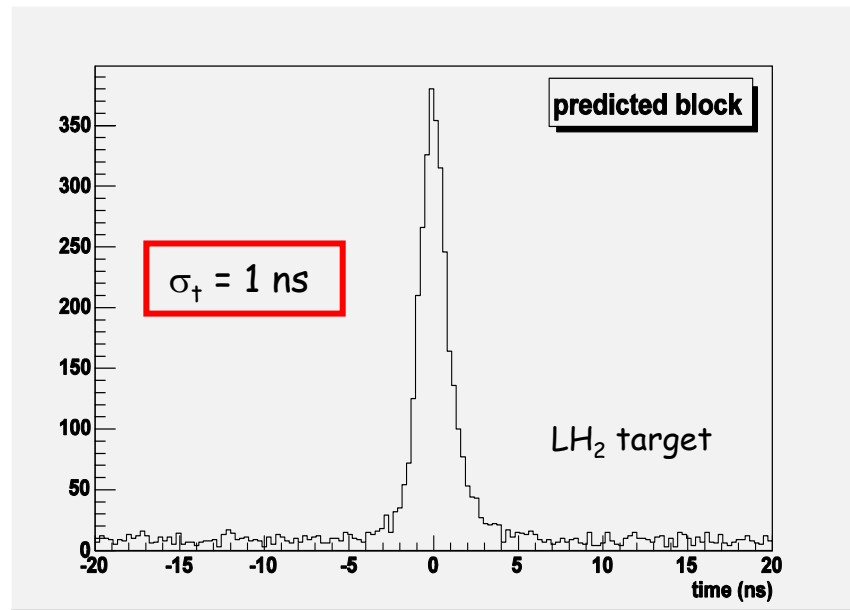
An **ey coincidence** freezes the **Analog Ring Sampler** and launches an accurate signal digitization in terms of **128 samples of 1 ns duration**

Off-line wave form analysis

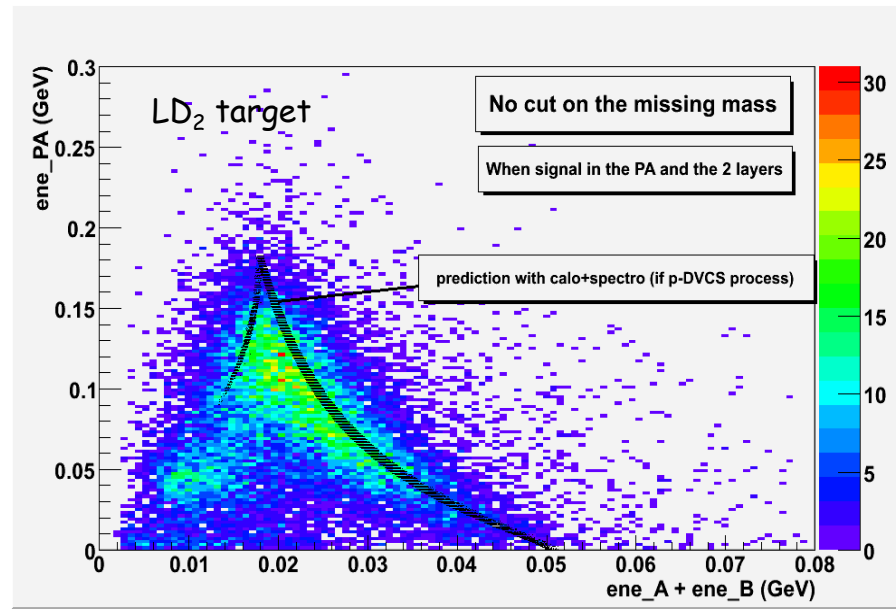
→ **Minimum separation time of 4 ns**

Experimental Features

Hadronic Calorimeter



Coincidence time spectrum of the Proton Array when looking at the **block predicted** from the scattered electron and the real photon

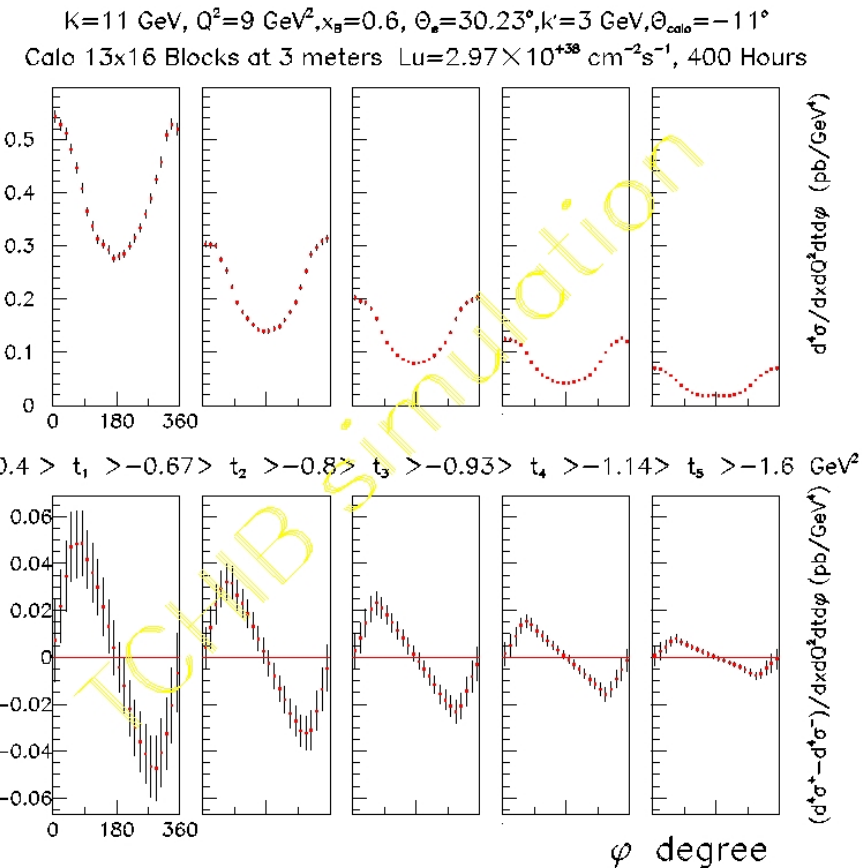
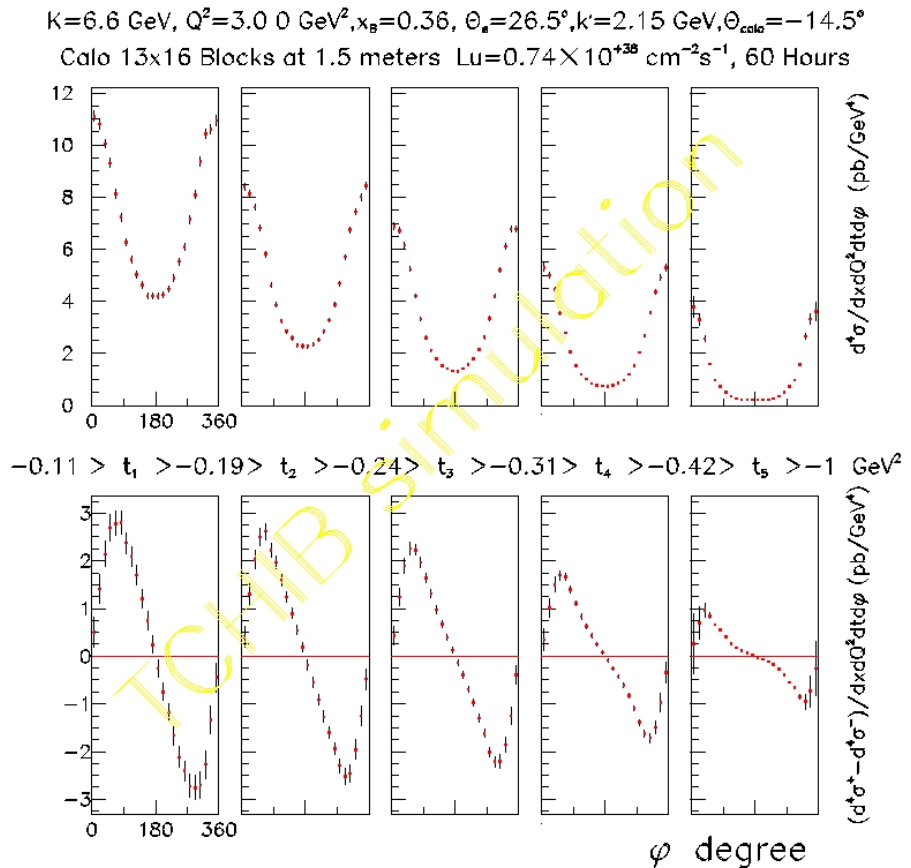


Energy deposit in the Proton Array and in the Tagger when requiring in-time signals in each detector

Good operation of the **Tagger** and **Proton Array** assembly which are used in a **logic** based analysis to **check exclusivity**

Neutron → **001** Proton → **111**

Experimental Features



Measuring $s^{\text{DVCS,I}}$ and $c^{\text{DVCS,I}}$ harmonic coefficients linked to linear combinations of GPDs and of integrals of GPDs